Indonesian Journal of Electrical Engineering and Computer Science
Vol. 41, No. 3, March 2026, pp. 845~858
ISSN: 2502-4752, DOI: 10.11591/ijeecs.v41.i3.pp845-858

Thermal effects of curing parameters on the natural frequency of GNP/Ag ink composites

Khirwizam Md Hkhir[1], Nor Azmmi Masripan[2], Cholatee Photong[3], Alan Watson[4], Mohd Azli Salim[2]
[1]Jabatan Kejuruteraan Mekanikal, Politeknik Ungku Omar, Perak, Malaysia
[2]Fakulti Teknologi dan Kejuruteraan Mekanikal, Universiti Teknikal Malaysia Melaka, Hang Tuah Jaya, Malaysia
[3]Faculty of Engineering, Mahasarakham University, Maha Sarakham, Thailand
[4]Power Electronics and Machines Centre, The University of Nottingham, Nottingham, United Kingdom

Article Info

Article history:

Received Nov 6, 2025
Revised Nov 12, 2025
Accepted Dec 13, 2025

Keywords:

Curing temperature
Curing time
GNP/Ag Conductive Ink
Natural frequency
Resistivity

ABSTRACT

This research examines how curing temperature and duration influence the electrical and mechanical behavior of hybrid graphene nanoplatelet and silver (GNP/Ag) conductive ink. The ink was formulated from GNPs, silver flakes and silver acetate printed on copper substrates, then cured 240 °C, 250 °C, and 260 °C for one to three hours. Electrical resistance was measured using a Two-Point probe, while natural frequency was obtained from experimental modal analysis (EMA) on stainless-steel (SUS304) cantilever beams laminated with printed ink. The results show that the higher curing temperature and longer curing time reduce resistivity and increase natural frequency, with the best performance observed at 260 °C for 3 hours (8.4×10^{-6} Ω.m and a 4.2 Hz increase). These findings confirm that a direct relationship between conductivity and stiffness, where conditions that promote stronger particle bonding also raise structural rigidity. The main contribution of this research is the joint evaluation of curing effects on both electrical and vibrational responses, offering a combined electro-mechanical perspective that is not often explored in GNP/Ag ink research. The results provide practical guidance for selecting curing conditions based on the required balance between conductivity and mechanical stability in flexible and stretchable electronic applications.

Corresponding Author:

Mohd Azli Salim
Fakulti Teknologi dan Kejuruteraan Mekanikal, Universiti Teknikal Malaysia Melaka
Hang Tuah Jaya, 76100 Durian Tunggal, Melaka, Malaysia
Email: azlisalim@utem.edu.my

1. INTRODUCTION

Conductive inks have emerged as a transformative material in the field of printed electronics, enabling the development of flexible, lightweight and cost-effective electronic devices. These inks are widely utilized in flexible electronics for applications such as sensors, antennas, and interconnects [1]-[3]. Typically, conductive inks consist of conductive fillers, such as silver (Ag) nanoparticles, carbon- based materials which are graphene and carbon nanotubes (CNT) or conductive polymers, where it is dispersed within a solvent or polymer matrix. This study focuses on a hybrid ink formulation comprising graphene nanoplatelets (GNPs) and Ag particles. The GNPs, when used as fillers in conductive inks have demonstrated the ability to enhance both electrical and mechanical properties of polymer-based systems, making them highly suitable for advanced electronic applications [4]. The integration of GNPs with Ag nanoparticles has been shown to further improve electrical conductivity due to a synergistic effect, which enhances inter-particle connectivity

and reduces electron scattering [5]-[7]. This hybrid approach holds significant promise for the development of high-performance conductive inks for flexible and stretchable electronic devices.

The performance of conductive inks is closely linked to the curing conditions. Temperature and curing condition influence solvent evaporation, particle sintering and interfacial bonding between the printed layer and the substrate. Several studies have shown that higher curing temperatures and longer curing times enhance particle sintering and improve electrical conductivity. Bakar *et al.* [8] demonstrated that optimized thermal exposure promotes more uniform sintering in hybrid GNP/Ag inks. Chen *et al*. [9] further explained the thermal mechanisms that govern solvent removal and particle sintering in nanoparticle based conductive inks. Similar trends were observed in in-situ curing studies by Janda *et al.* [10], while Merilampi *et al.* [11] reported improves electrical performance in silver-based inks when sufficient thermal energy is supplied. Additional work on polymer substrates has confirmed that curing conditions directly influence the formation of conductive pathways [12] and recent findings by Salim *et al.* [13] highlights the sensitivity of GNP/Ag systems to changes in curing temperature. Although these studies provide valuable insight into electrical behavior, most examine curing effects only from an electrical perspective and seldom consider their mechanical implications.

Mechanical behavior is also important especially for devices exposed to bending, cyclic loads or vibration. Natural frequency is usually parameter for assessing stiffness and structural integrity in thin films and laminated composites also can affect the performance of devices such as resonators, sensors and frequency selective surface. Deng *et al*. [14] stated that conductive ink-based frequency selective surfaces rely on stable resonance behavior to maintain wideband absorption. Tu *et al.* [15] also showed that variations in stiffness and film uniformity influence resonant measurements in printed conductive films at microwave frequencies. More recent studies, such as those by Summers *et al.* [16], stated how ink microstructure affects RF performance, reinforcing the importance of mechanical stability in printed conductors. Hybrid graphene silver used in flexible and stretchable electronics face similar challenges by [5], who emphasized that mechanical integrity is important for devices subjected to repeated deformation. Despite its relevance, natural frequency analysis is still uncommon incorporated in conductive ink studies. Existing research does not examine how curing conditions simultaneously influence electrical and mechanical behavior in hybrid GNP/Ag conductive inks.

This gap is significant because thermal processing can affect both conductivity and stiffness through changes in microstructure. Although several works discuss curing and heat related effects conceptually [8], [9], current studies do not address the combined electro-mechanical response of GNP/Ag conductive inks under different curing temperatures and times. While many studies show that increasing of the curing temperature and time can improve conductivity, much less has been done to understand how the same curing conditions affect mechanical stiffness, especially when viewed through natural frequency. This leaves an important gap because devices using printed conductive layers experience bending, vibration and cyclic loading in real applications. A combine constraint that connects electrical and mechanical responses under identical curing conditions has not been established for GNP/Ag hybrid inks.

This study responds to that gap by investigating how curing temperature and curing time affect both the electrical resistance and natural frequency of printed GNP/Ag conductive ink. The hypothesis is that higher curing temperatures and longer curing durations enhance heat transfer during curing, leading to stronger paricle sintering, lower resistivity and increased stiffness. Therefore, this study aims to examine how curing temperature and duration influence both the electrical and natural frequency of printed GNP/Ag conductive ink and to identify curing conditions that offer a balanced improvement in electrical and mechanical performance in flexible and stretchable electronic devices.

2. METHOD

This study focuses on the formulation and processing of a conductive ink composed of a hybrid mixture of three conductive fillers which are GNPs with a particle size of 25 µm, Ag nanoparticles with a particle size of 10 µm, and SA. Besides, ethanol was used as the primary chemical solvent, while 1-butanol and terpineol served as organic solvents and binders to support dispersion and film formation. The sample preparation process involved several key stages, including ink formulation, mixing of powder and paste components, stencil-based ink printing, thermal curing and subsequent characterization of the cured samples which the flow illustrates in Figure 1.

2.1. Formulation of GNP/Ag conductive ink composite

The primary formulation of conductive ink consists of two main components, such as conductive fillers and a binder system. The fillers are responsible for electrical conductivity, while the binder ensures proper dispersion and cohesion of all constituents within the ink. In this study, the formulation of the

GNP/Ag conductive ink composite utilized a specific ratio of filler loading and solvent, as detailed in Table 1 for one sample set. This formulation approach was adapted from the method described by [17] for developing hybrid conductive inks. The required quantities of each component were accurately weighed using a digital scale and placed in a clean beaker for subsequent mixing and processing.

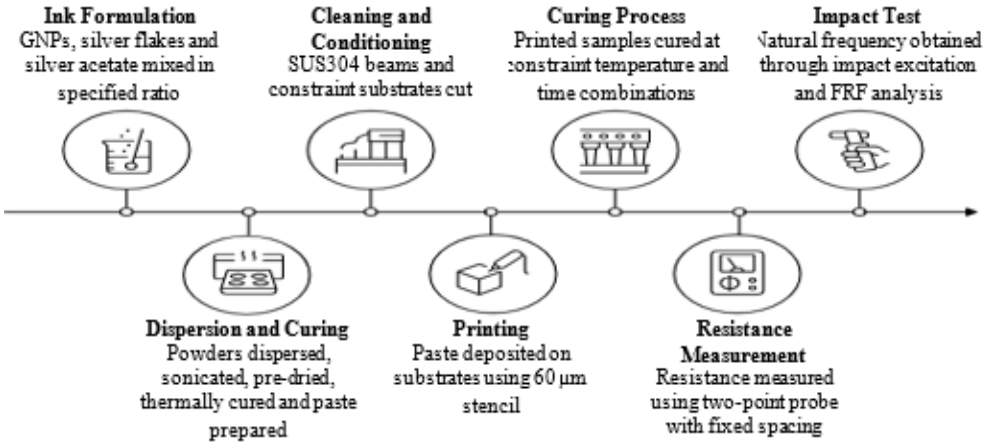

Figure 1. Experiment workflow for GNP/Ag conductive ink composite test

Table 1. Composition of GNP/Ag conductive ink composite for 1 sample set

GNP (g)	Ethanol (ml)	Silver flake, Ag (g)	Silver acetate, SA (g)	Ratio 1-butanol: Terpineol
0.005	5	0.4292	0.042	3:3

The formulation was designed to balance electrical conductivity with good mechanical stability. Silver flake were used as the main conductive components because it form the bulk of the electron pathways. A small amount of GNP was added to reinforce the printed layer and improve particle to particle contact. Silver acetate was included as well, since it breaks down during curing and produces additional silver that helps the particle bond more effectively. The mass ratio used for GNPs, silver flakes, and silver acetate (about 0.005: 0.4292: 0.042 per single set batch) follows earlier findings showing that hybrid systems benefit from this composition range [13], [18].

2.2. Mixing process

The components were combined to produce a uniform mixture suitable for use as conductive ink in test sample printing. Achieving a homogeneous dispersion of GNPs, Ag and solvents is essential for ensuring consistent filler distribution, which directly influences electrical conductivity and thermal behavior. A magnetic stirrer was used to facilitate uniform mixing. According to the formulation for a single sample set, the procedure was scaled up to prepare 18 sets which are specified quantities for one set were multiplied by 18 to produce a larger batch of conductive paste.

For the preparation of this 18-set batch, 0.090 g of GNPs was first dispersed in 90 ml of ethanol in a small beaker. The beaker was covered with aluminum foil to minimize solvent evaporation. By promoting effective dispersion of the GNPs particles, the mixture was placed in an ultrasonic bath for 10 minutes, following procedures adapted from [18]. After the initial dispersion, 7.7256 g of SF were added to the GNPs/ethanol mixture, and the combined solution underwent further sonication for 1 hour. During this process, the ultrasonic bath was operated at a nominal amplitude of 40 kHz to promote effective particle breakup. The mixture was inspected visually during and after sonication and no sedimentation or particle clustering was observed indicating stable dispersion. The mixture was also checked under an optical microsope, which showed no large agglomerates. These observations confirmed that GNPs and silver-based fillers were well dispersed before moving on to the next step. Studies have shown that such prolonged sonication may induce structural modifications in graphene-based materials, such as introducing defects that could affect both electronic and thermal properties [19], [20]. Although prolonged sonication can introduce structural changes, the dispersion checks confirmed that the particle network remained uniform and stable throughout processing.

During this process, the dispersibility of GNPs in ethanol and its interaction with Ag nanoparticles were observed as shown in Figure 2. The resulting homogeneity is critical not only for achieving consistent electrical performance but also for enhancing heat transfer efficiency during the curing stage. A well-dispersed ink ensures uniform thermal conductivity across the printed layer, promoting even heat distribution during curing. This leads to more effective sintering of conductive particles, better solvent evaporation, and stronger interfacial bonding with the substrate, which contributes to improved electrical conductivity and mechanical stiffness. Figure 2(a) illustrates the sonication process using an ultrasonic bath.

Next, 0.756 g of SA was added to the previously sonicated mixture, followed by an additional 1 hour of sonication to ensure thorough dispersion of all conductive components. The mixture was then heated on a hot plate at 70 °C while being stirred at 200 rpm using a magnetic stirrer to aid the evaporation of excess ethanol, as illustrated in Figure 2(b). This low temperature pre-drying step promotes uniform distribution of conductive particles and initiates early solvent removal, which supports better heat transfer during subsequent high temperature curing.

After the stirring and drying process, the mixture was transferred to a small white porcelain beaker and thermally cured in an oven at 250 °C for 1 hour. This curing step not only solidifies the composite but also significantly improves thermal conductivity by enhancing particle sintering and reducing interfacial voids. As a result, the heat transfer characteristics of the ink are improved, ensuring more efficient energy distribution during device operation. Once cooled, the cured composite was finely ground to produce a uniform powder. This powder was stored in a clean container for paste preparation.

For the preparation of the GNP hybrid paste, 9.36 g of the cured powder was weighed and placed in a small container. Then, 54 drops of 1-butanol and terpineol were added to serve as organic binders, improving the paste's consistency and printability as shown in Figure 3. The mixture was blended thoroughly using a mixing machine to create a homogeneous conductive ink paste. This final paste not only supports electrical conductivity but also contributes to enhanced heat dissipation in printed electronic devices depending to the optimized microstructure and thermal pathways established during the curing process.

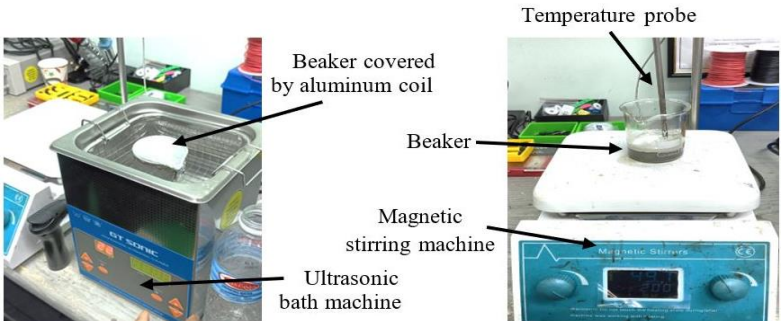

Figure 2. Conductive ink preparation process: (a) sonication process and (b) stirring process

Figure 3. 1-butanol and terpineol dropping process

2.3. Printing process

For the method of printing, this research used a manual mesh stencil printing whose thickness at 60 µm while thin copper films would have served as substrates. This involved putting a substrate under this mesh stencil followed by pasting it with a grid size of 3 mm×3 mm like in Figure 4. The paste was printed on

the five selected points on the substrate strip, using a squeegee, until it was visible as illustrated in Figure 5. After printing, there should be cleaning of the mesh stencil and this should be done for all the 18 set to proceed to curing process.

Figure 4. Printing process on 60 µm mesh stencil thickness

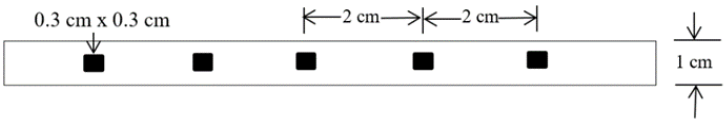

Figure 5. Schematic diagram for printing points

2.4. Curing process

The curing process is a critical post-treatment step performed after the conductive ink has been printed onto the substrate. This process enhances the adhesion between the conductive fillers and the binder, while also strengthening the bonding between the ink and the substrate surface. In this study, curing was carried out using the UF55 universal oven, which features a highly efficient heating system that ensures uniform heat distribution and stable temperature conditions throughout the chamber. The printed samples were placed on a tray and subjected to curing under various temperature and time conditions, as detailed in Table 2. Recent studies on hybrid GNP/Ag conductive inks shows the effective particle sintering and silver reduction occur in the 230-280 °C range, where solvent removal and neck formation between particles become more active [8], [9], [12]. Based on these findings, the curing temperatures of 240 °C, 250 °C, and 260 °C were selected to fall within the established sintering for GNP/Ag composite inks. The oven was preheated for 20 minutes and run with a steady internal airflow, which helped keep the temperature uniform and ensured that every sample received consistent heat exposure.

The uniform thermal environment provided by the oven promotes consistent sintering of conductive particles, resulting in denser microstructures and improved interfacial contact between components. As a result, the heat transfer characteristics of the printed ink layer are significantly improved, which is beneficial for applications where thermal dissipation and stability are crucial, such as in flexible electronics and high-frequency devices. Following the curing process, all samples were allowed to cool naturally to room temperature to complete the thermal stabilization phase.

Table 2. Sample preparation

Sample	Number of samples	Curing temperature (°C)	Curing time (hours)
S1	2	240	1
S2	2	240	2
S3	2	240	3
S4	2	250	1
S5	2	250	2
S6	2	250	3
S7	2	260	1
S8	2	260	2
S9	2	260	3

2.5. Resistance and resistivity analysis

The resistance measurement was performed according to IEEE standard 118-1978 using a two-point probe and it is measured the resistance at each conductive ink. Data reading was taken by tapping specific

positions on each substrate point as shown in Figure 6. The probe tips were applied with constant contact pressure to reduce variation caused by contact resistance and the electrode spacing was kept at 3 mm for all samples to ensure consistent measurement conditions. For each curing condition, two printed samples were tested and every reported value represents the mean of three repeated measurement. The average value of each sample containing five printed ink readings will be calculated.

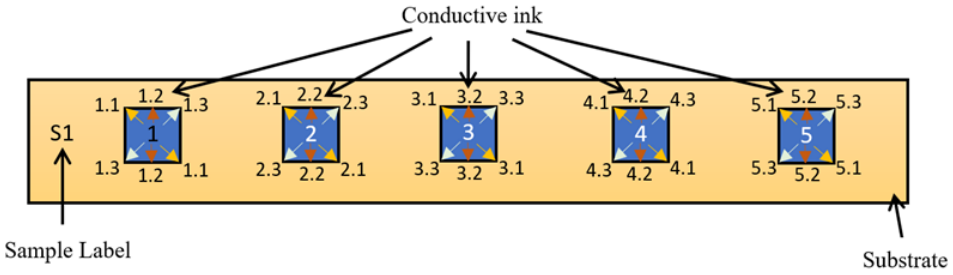

Figure 6. Schematic diagram of printed ink with testing points

From the reading of resistance, the conductive ink resistivity is defined as follows in (1):

$$\text{Resistivity, } \rho = \frac{R}{L} \times A \quad (1)$$

where R is the measured resistance, L is the length of the current path, A is the area of the printed conductive ink defined as follows in (2).

$$\text{Area, } A = w \times L \quad (2)$$

where, w is the thickness of mesh stencil.

2.6. Natural frequency measurement

In this study, natural frequency values were obtained from experimental modal analysis (EMA), following the ASTM E756 standard, as illustrated in Figure 7. The test specimens consisted of stainless-steel (SUS 304) cantilever beams with conductive ink printed on their surface under varying curing temperatures and curing times. The SUS 304 stainless steel was chosen as the substrate because of its high stiffness-to-mass ratio, which ensures well-defined natural frequencies with minimal damping effects [21]. The properties and dimensions of the SUS 304 beams used in this investigation are presented in Table 3 and Figure 8.

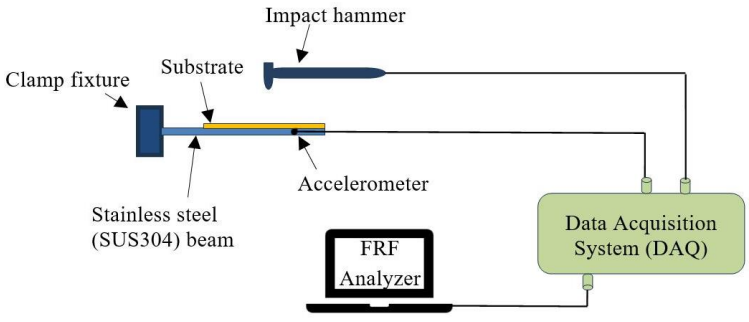

Figure 7. Test setup for EMA

Table 3. The stainless steel (SUS 304) beam specification

Material	Stainless-steel (SUS 304)
Young's Modulus, E	200 GPa
Density, ρ	9,730 kg/m^3
Dimension, length, l × width, b × thickness, h	200 mm×10 mm×3 mm

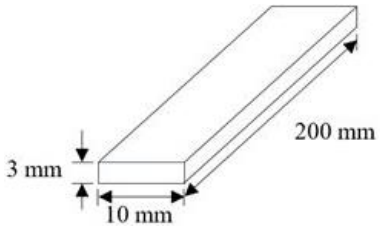

Figure 8. Stainless steel (SUS 304) dimension

The SUS304 beam was laminated with the printed GNP/Ag conductive ink on different substrate constraints was fixed as a cantilever with one end fully clamped in a rigid vise. A soft-tip impact hammer was used to excite the beam and generate a clear impulse response. The lightweight miniature accelerometer with reference sensitivity about 10.34 mV/g is used to acquire displacement signals placed. The data acquisition system (DAQ) simultaneously records the time-domain force and acceleration signals, which are then processed using a fast fourier transform (FFT) algorithm to convert them into frequency spectra. By calculating the frequency response function (FRF), which is the ratio of the output (acceleration) spectrum to the input (force) spectrum, the system determines the natural frequencies of the structure. The peaks in the FRF curve represent the natural frequency of SUS 304 beam laminated with specimens' substrate. In this study, the analysis focused on the first natural frequency, which corresponds to lowest resonant mode of the structure and provides the most meaningful indication of its stiffness [22]. Each two sample with different curing conditions was tested three times to check repeatability and the average value was used as the final frequency. The repeated measurement showed consistent variation within ±0.5 Hz, indicating stable and reliable data across all curing conditions.

At first, the experimental reading of natural frequency of stainless-steel beam without specimens' substrate was observed properly and compared with theoretical calculation. In vibration analysis to ensure the experimental reading precise, comparing experimental reading with theoretical is essential to leads more accurate predictions and better understanding of the system's dynamic behavior [22]. The theoretical natural frequency, f_n get by using (3):

$$\text{Natural frequency, } f_n = \frac{\omega}{2\pi}\beta_1^2\sqrt{\frac{EI}{\rho AL^4}} \quad (3)$$

where, E = Young's modulus of the beam material (Pa), I = Area moment of inertia of the beam cross-section (mm⁴), ρ = Density of the beam material (kg/m³), A = Cross-sectional area of the beam (m²), L = Length of the beam (m) and β_1 = mode of shape (depend on boundary condition), β_1 = 4.694 (cantilever). The natural frequency readings of the samples substrate with different constraints were then finalized by taking differential precise measurements between of the natural frequency of the SUS 304 beam with the sample substrate and the natural frequency readings of the beam without the sample substrate.

3. RESULTS AND DISCUSSION

3.1. Resistance and resistivity of GNP/Ag highly thermal at room temperature

The two-point probe experiment was conducted to measure the electrical resistance of the test samples at room temperature. For each conductive ink sample, resistance measurements were taken at five specific points using the method, yielding a total of fifteen data points per sample. Table 4 presents the measured average resistance, resistivity, and standard deviation values. Each data point represents the mean of three readings across two samples. The standard deviation for most conditions remained below 5%, indicating low measurement variation. Sample S9, cured at 260 °C for 3 hours, demonstrated the best electrical conductivity, with the lowest resistance and resistivity values of approximately 0.1400 Ω and 8.400×10^{-6} Ω·m respectively. This significant improvement can be attributed to enhanced heat transfer during the curing process. Fundamentally, efficient thermal conduction enables uniform temperature distribution throughout the ink layer, which accelerates the sintering process, where atomic diffusion at particle interfaces forms strong bonds between GNPs and Ag nanoparticles. According to heat transfer principles, higher temperature and longer exposure increase thermal energy input, promoting particle neck growth and dispersion. This reduces microstructural voids and improves inter-particle connectivity, thereby lowering electrical resistance and enhancing conductivity.

Table 4. The result of resistance and resistivity for sample test

Sample	Average Resistance, R (Ω)	Average Resistivity, ρ (Ω.m)	Standard deviation of resistance
S1	0.1423	8.5400e-06	2.7386e-03
S2	0.1420	8.5200e-06	1.3944e-03
S3	0.1420	8.5200e-06	1.3944e-03
S4	0.1422	8.5333e-06	1.1111e-03
S5	0.1420	8.5200e-06	2.5386e-03
S6	0.1420	8.5200e-06	2.5386e-03
S7	0.1410	8.4600e-06	1.9003e-03
S8	0.1406	8.4400e-06	9.1287e-04
S9	0.1400	8.4000e-06	1.1785e-03

Conversely, samples cured at lower temperatures or shorter durations, such as S1 and S2, showed higher resistivity and resistance values. This outcome is consistent with incomplete curing resulting from insufficient heat transfer. When thermal energy is limited, the temperature gradient within the ink layer becomes non-uniform, reducing effective heat conduction. Poor heat transfer slows solvent evaporation and re-stricts polymer crosslinking, leaving residual voids and defects that disrupt conductive pathways. These microstructural imperfections cause increased electron scattering and reduce electrical conductivity. Thus, the fundamental heat transfer mechanisms during curing critically influence the formation of continuous conductive networks necessary for optimal electrical performance.

Additionally, variability in resistance measurements across multiple points,reflected in the standard deviation and it is also relating to heat transfer efficiency. Sample S1 showed the highest standard deviation which is 2.7386×10^{-3}, indicating inconsistent microstructure and thermal processing. In contrast, sample S8 exhibited the lowest standard deviation, 9.1287×10^{-4}, reflecting more uniform heat distribution and consistent particle sintering during curing. From a heat transfer standpoint, this consistency suggests that improved thermal conduction results in homogeneous curing conditions, yielding stable and reproducible electrical properties.

Therefore, the fundamental principles of heat transfer, particularly thermal conduction are central to controlling the curing process and the resulting electrical properties of GNPs/Ag conductive inks. Efficient heat transfer ensures uniform temperature profiles that facilitate solvent removal, particle sintering and polymer crosslinking, all of which contribute to the formation of a dense and highly conductive network. Optimizing curing parameters to maximize heat transfer thus plays a crucial role in achieving low-resistance, mechanically stable and reliable printed electronic materials.

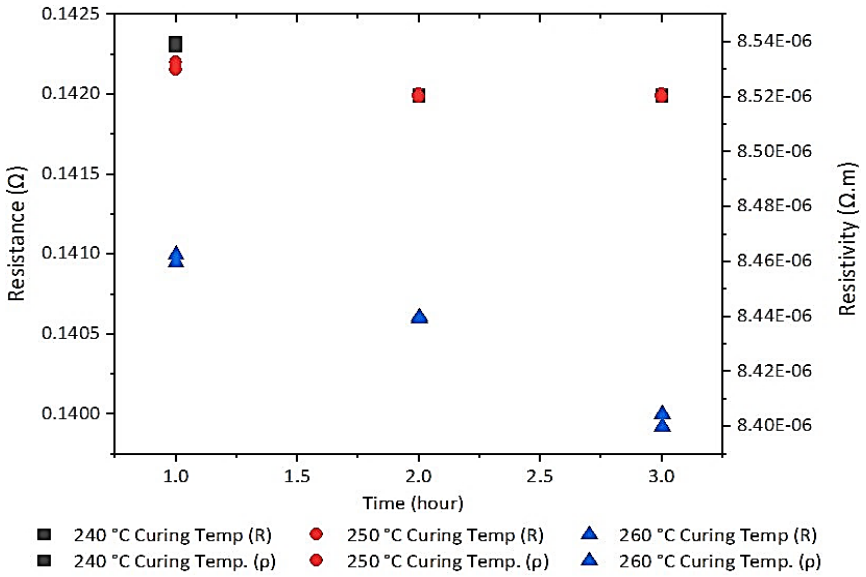

Figure 9. Resistance and resistivity for difference curing temperatures and times

Figure 9 illustrates the trends in resistance and resistivity across various curing temperatures and durations, showing a steady decrease in both parameters as temperature and time increase. This trend reflects the fundamental role of heat transfer, specifically thermal conduction in delivering consistent thermal energy to the conductive ink. Efficient heat transfer ensures uniform temperature distribution throughout the material, which accelerates the curing process by providing the necessary energy for molecular and atomic rearrangements. As a result, increased thermal energy improves electrical conductivity by enhancing particle bonding and reducing defects within the composite.

According to Xia *et al.* [4] and Bakar *et al.* [8], higher curing temperatures maintained over longer durations improve the electrical performance and durability of GNPs/Ag composites [23]. From a heat transfer perspective, this occurs because the enhanced thermal gradient facilitates the removal of residual solvents and impurities through evaporation and diffusion. The effective transfer of heat drives these processes, which reduces electron scattering caused by impurities and minimizes contact resistance between particles. Thus, the interplay between thermal energy delivery and mass transport mechanisms underpins the improvement in electrical properties observed with elevated curing parameters.

Furthermore, increased curing temperatures provide sufficient thermal energy to enable the conductive fillers, GNPs and Ag nanoparticles to overcome the intermolecular forces restricting their mobility within the polymer matrix. This phenomenon is fundamentally related to heat-induced particle diffusion and reorientation, which are governed by temperature-dependent kinetics described by Arrhenius-type behavior. The enhanced heat transfer promotes filler alignment and densification, resulting in a more continuous and tightly packed conductive network. This improved connectivity effectively reduces insulating gaps and creates more direct conductive pathways, thereby significantly lowering resistance and resistivity.

Moreover, the extended application of heat during curing facilitates structural rearrangements and improved interfacial bonding within the composite, contributing to enhanced thermal stability. The heat transfer mechanisms involved allow the composite to achieve a more stable microstructure that can maintain its conductive properties under mechanical stress and environmental changes. This thermal stability is crucial for reliable performance in flexible electronic applications, where consistent electrical behavior is essential despite bending or temperature fluctuations.

3.2. Natural frequency of highly thermal GNP/Ag

EMA represents a strong method which researchers use to determine structural dynamics parameters through physical testing. The SUS 304 beam receives measurement through strategically placed accelerometers while an soft-tip impact hammer delivers a known excitation force. The collected data undergoes FFT analysis in the frequency domain to generate FRFs. The FRFs show how the structure behaves at different input frequencies which helps identify essential dynamic properties as illustrated in Figure 10.

The vertical axis of the FRF graph in Figure 10 shows the output response amplitude relative to the input force through decibel (dB) measurements. The FRFs graph shows a steep rise at frequencies with the most prominent peak occurring at 384.4 Hz which indicates the natural frequencies of the structure where the beam resonates most strongly. The FRFs plot shows this peak because of the fundamental principles of mechanical system vibration and resonance. The structure absorbs input energy most efficiently when its natural frequency matches its stiffness and mass properties. In this study, the experimental value of 384.4 Hz functions as a baseline to assess the beam frequency response after adding a substrate printed with conductive GNPs/Ag ink to its surface.

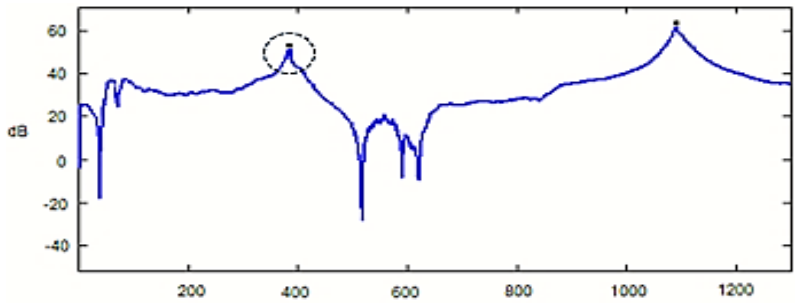

Figure 10. Peak natural frequency in FRF stainless-steel beam at 384.4 Hz

Before using the experimentally obtained natural frequency values as a reference for further measurements, it is essential to validate them by comparing with theoretical calculations. As noted by Luo and Yang [21], such comparisons are critical to ensuring the accuracy and reliability of experimental data. The natural frequency of a cantilever beam is fundamentally determined by its material properties, such as stiffness and density, geometry which are length and cross-sectional shape and boundary conditions. Classical beam theory, based on the Euler-Bernoulli model, describes how these factors influence the beam's vibrational behavior, assuming small deformations and elastic response [24].

Theoretical predictions of natural frequency rely on the beam's stiffness, how resistant it is to be bending and its mass distribution. A stiffer beam or one with less mass typically exhibits a higher natural frequency, while a heavier or more flexible beam vibrates at lower frequencies. Validating experimental results against these theoretical values ensures that the assumptions made about material homogeneity, geometry, and boundary constraints are accurate, and that the experimental setup is functioning correctly.

This comparison not only enhances the precision of the dynamic system model but also provides confidence that the experimental data can serve as a dependable baseline for further studies involving the SUS 304 beam coated with GNPs/Ag conductive ink. Table 5 presents the natural frequency values obtained experimentally and theoretically for the bare stainless-steel beam. The experimental frequency was measured at 384.4 Hz, while the theoretical value was calculated at 381.3 Hz, resulting in a minor error of 3.1 Hz or 0.8%. This close agreement confirms the validity of the experimental setup and supports the assumptions in the theoretical framework, reinforcing the credibility of the subsequent analysis.

Table 5. The result of natural frequency for stainless-steel without samples

Experimental natural frequency, f_n (Hz)	Theoretical natural frequency, f_n (Hz)	Error percentage (%)
384.4	381.3	0.8

Table 6 presents the measured natural frequencies obtained from the first peak in the FRFs of multiple beam specimens. Each beam was fabricated from SUS 304, laminated with a copper substrate and printed with conductive GNPs/Ag ink, then cured under varying conditions. The natural frequency of the unmodified beam is 384.4 Hz and shown in Table 5, was used as a baseline to isolate the influence of the added substrate and printed ink layers. This approach allows for a clearer understanding of how the conductive ink and curing conditions affect the overall dynamic behavior of the beam. The recorded frequency shifts varied from as little as 1.00 Hz up to 4.20 Hz, illustrating how even slight modifications to the material composition and structure can significantly influence the dynamic response of a beam. Natural frequency shifts were consistent across samples, with variations below ±0.5 Hz. These shifts arise because natural frequency is highly sensitive to changes in the beam's mass and stiffness distribution, which is two fundamental parameters governing vibration behavior. Different curing parameters likely altered the micro-structure and bonding within the ink layer, leading to variations in material properties and thus either increasing or decreasing the beam's natural frequency. This pattern underscores how subtle changes at the microscale level can propagate into measurable macroscopic effects on mechanical performance.

Table 6. The result of natural frequency for sample test

Sample	Experimental natural frequency, f_n (Hz)	Experimental natural frequency, f_n of stainless-steel beam (Hz)	Sample natural frequency, f_n (Hz)
S1	385.4	384.4	1.00
S2	385.9	384.4	1.50
S3	386.2	384.4	1.80
S4	386.1	384.4	1.70
S5	387.2	384.4	2.80
S6	387.1	384.4	2.70
S7	387.8	384.4	3.40
S8	388.3	384.4	3.90
S9	388.6	384.4	4.20

From a vibration mechanics perspective, the shift in natural frequency is explained by the interplay between added mass and increased stiffness introduced by the laminated layers of substrate and printed ink. While adding mass to a structure tends to lower its natural frequency increased inertia resisting motion, an increase in stiffness tends to raise the natural frequency by making the structure more resistant to deformation. The balance between these competing effects depends largely on the quality of the curing

process. Higher curing temperatures and longer curing times promote enhanced sintering of conductive particles and stronger interfacial bonding within the ink layer. This improved microstructure results in increased rigidity and better adhesion, which enhances the overall stiffness of the composite beam and may outweigh the effect of added mass, leading to a net increase in natural frequency.

The observed trend of increasing natural frequency with more effective curing conditions highlights the critical role of processing parameters in determining the mechanical behavior of printed conductive layers. These findings emphasize that curing not only affects electrical conductivity but also significantly impacts the mechanical integrity and dynamic performance of the printed ink. Frequency-based characterization methods prove to be highly sensitive tools for detecting changes in structural properties and are particularly valuable in the development and quality control of flexible electronics and thin-film materials used in structural health monitoring. This sensitivity is rooted in the fundamental principle that a structure's vibrational characteristics directly reflect its physical and mechanical state.

Figure 11 illustrates a clear inverse relationship between electrical resistance and natural frequency in GNPs/Ag conductive ink composites, where a reduction in resistance corresponds to an increase in natural frequency. This phenomenon can be fundamentally explained by the microstructural evolution within the ink during the curing process and the intrinsic connection between electrical and mechanical properties of the composite. Electrical resistance depends largely on the formation of continuous conductive pathways created by the fillers such as GNPs and Ag nanoparticles. When the curing parameters such as temperature and time are properly controlled, effective heat transfer supplies thermal energy that promotes solvent evaporation, particle sintering and improved dispersion. These heat-driven processes enhance the connectivity between conductive fillers, enabling electrons to travel more freely and thereby reducing resistance.

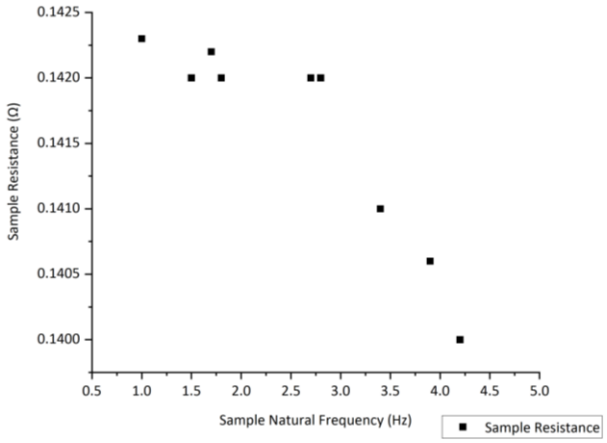

Figure 11. The relationship between resistance value and natural frequency

Simultaneously, the microstructural changes that lower resistance also affect the mechanical properties, particularly stiffness, which governs the natural frequency of the material. The natural frequency reflects how quickly a material or structure vibrates, and it is influenced by the ratio of stiffness to mass. As curing improves bonding between particles and densifies the composite, stiffness increases. Heat transfer ensures that the curing temperature is uniformly distributed, allowing the ink layer to develop consistent mechanical integrity. With increased stiffness, the natural frequency rises because the structure becomes more resistant to deformation and vibrates at higher frequencies. Thus, the inverse correlation between resistance and natural frequency arises because the thermal energy applied during curing simultaneously improves conductive pathways and strengthens mechanical rigidity.

Heat transfer is a critical element in this process because it dictates how thermal energy moves through the conductive ink and its substrate. Primarily driven by conduction in solid materials, heat must be uniformly transmitted to ensure that all regions of the ink receive sufficient energy for chemical reactions such as cross-linking and sintering to proceed effectively. Uneven heat distribution leads to temperature gradients, causing incomplete curing in some regions, which results in residual solvents, voids, and weak particle adhesion. These defects disrupt electron flow, increasing electrical resistance, and weaken structural stiffness, reducing the natural frequency. Conversely, effective heat trans-fer minimizes such imperfections by maintaining a consistent curing environment, thereby optimizing both electrical conductivity and mechanical stability.

The fundamental principle of heat conduction asserts that thermal energy moves from regions of higher temperature to lower temperature until thermal equilibrium is reached. In the context of curing conductive inks, ensuring steady heat flow facilitates the rearrangement and bonding of conductive particles into a dense, intercon-nected network. This structural refinement lowers the energy barriers for electron transport and enhances the composite's mechanical performance. The interdependence of electrical and mechanical characteristics governed by heat transfer highlights the importance of controlling curing conditions precisely.

Practically, this relationship means that by manipulating curing temperature and duration, thereby controlling heat transfer, manufacturers can tailor the electrical resistance and natural frequency of conductive inks to meet specific functional requirements. This is particularly important in flexible and stretchable electronics, where consistent conductivity and mechanical resilience under deformation are essential for device performance and durability. The curing process, mediated by heat transfer, thus serves as a fundamental mechanism that shapes the final properties of the conductive ink, ultimately influencing its suitability for advanced electronic applications.

4. CONCLUSION

This study evaluated the combined electrical and mechanical response of GNP/Ag hybrid confuctive ink under different curing conditions. Higher curing temperatures and longer curing effect reducing of resistivity while increasing natural frequency, confirming that improved particle densification benefits both conductivity and stiffness. The curing range of 260 ºC for 3 hours provided the best balance between the two responses. The main contributions of this study is the joint assessment of electrical and vibration behavior, offering an integrated electro-mechanical perspective that is rarely explored in hybrid conductive ink studies. This approach helps clarify the interaction between particle sintering and structural rigidity. A limitation of the study is the use of SUS304 beam as the structural substrate, which provides a stiff base and may limit the visibility of changes that would be more pronounced in flexible substrates. Future work should include microstructural observation, such as scanning electron microspope (SEM), dynamic loading scenarios and extension to polymer-based substrates.

ACKNOWLEDGMENTS

Special thanks to the Advanced Academia-Industry Collaboration Laboratory (AiCL) and Fakulti Teknologi dan Kejuruteraan Mekanikal (FTKM), Universiti Teknikal Malaysia Melaka (UTeM) for providing the laboratory facilities.

FUNDING INFORMATION

The author(s) received no financial support for the research, authorship, and/or publication of this article.

AUTHOR CONTRIBUTIONS STATEMENT

This journal uses the Contributor Roles Taxonomy (CRediT) to recognize individual author contributions, reduce authorship disputes, and facilitate collaboration.

Name of Author	C	M	So	Va	Fo	I	R	D	O	E	Vi	Su	P	Fu
Khirwizam Md Hkhir	✓	✓	✓	✓	✓	✓		✓	✓	✓			✓	✓
Nor Azmmi Masripan		✓				✓		✓	✓	✓	✓	✓		
Cholatee Photong	✓			✓			✓			✓	✓		✓	
Alan Watson	✓			✓			✓			✓	✓		✓	
Mohd Azli Salim	✓	✓	✓	✓	✓	✓		✓	✓	✓		✓	✓	✓

C : **C**onceptualization
M : **M**ethodology
So : **So**ftware
Va : **Va**lidation
Fo : **Fo**rmal analysis
I : **I**nvestigation
R : **R**esources
D : **D**ata Curation
O : Writing - **O**riginal Draft
E : Writing - Review & **E**diting
Vi : **Vi**sualization
Su : **Su**pervision
P : **P**roject administration
Fu : **Fu**nding acquisition

CONFLICT OF INTEREST STATEMENT

Authors state no conflict of interest.

DATA AVAILABILITY

The data that support the findings of this study are openly available in [repository name] at http://doi.org/[doi], reference number [reference number].

REFERENCES

[1] E. Dimitriou and N. Michailidis, "Printable conductive inks used for the fabrication of electronics: an overview," *Nanotechnology*, vol. 32, no. 50, p. 502009, Mar. 2021, doi: 10.1088/1361-6528/abefff.

[2] M. A. Nalepa, "Graphene derivative-based ink advances inkjet printing of electrodes and senthereforers," *Biosenthereforers and Bioelectronics*, vol. 216, p. 116277, 2024, doi: 10.1016/j.bios.2024.116277.

[3] A. Koutsioukis, K. Vrettos, V. Belessi, and V. Georgakilas, "Conductivity enhancement of graphene and graphene derivatives by silver nanoparticles," *Applied Sciences*, vol. 13, no. 13, p. 7600, 2023, doi: 10.3390/app13137600.

[4] T. Xia, D. Zeng, Z. Li, R. J. Young, C. Vallés, and I. A. Kinloch, "Electrically conductive GNP/epoxy composites for out-of-autoclave thermoset curing through Joule heating," *Composites Science and Technology*, vol. 164, pp. 304–312, Jun. 2018, doi: 10.1016/j.compscitech.2018.05.053.

[5] Y. Z. N. Htwe and M. Mariatti, "Printed graphene and hybrid conductive inks for flexible, stretchable, and wearable electronics: Progress, opportunities, and challenges," *Journal of Science Advanced Materials and Devices*, vol. 7, no. 2, p. 100435, Feb. 2022, doi: 10.1016/j.jsamd.2022.100435.

[6] W. Li, J. Yan, C. Wang, N. Zhang, T. H. Choy, S. Liu, L. Zhao, X. Tao, and Y. Chai, "Molecule-bridged graphene/Ag for highly conductive ink," *Science China Materials*, vol. 65, pp. 2771–2778, 2022, doi: 10.1007/s40843-022-2064-8.

[7] Y. Z. N. Htwe and M. Mariatti, "Performance of water-based printed hybrid graphene/silver nanoparticles conductive inks for flexible strain senthereforer applications," *Synthetic Metals*, vol. 300, p. 117495, 2023, doi: 10.1016/j.synthmet.2023.117495.

[8] N. M. A. Bakar, N. M. A. Salim, N. nor A. Masripan, N. C. Photong, and N. C. K. Wayne, "Preparation of a new formulation of hybrid GNP/Ag conductive ink with a specific ratio of organic solvent," *Journal of Advanced Research in Micro and Nano Engieering*, vol. 25, no. 1, pp. 107–122, Dec. 2024, doi: 10.37934/armne.25.1.107122.

[9] R. T. Chen, H. Y. Liu, and P. Wong, "Thermal curing mechanisms in nanoparticle-based conductive inks for printed circuits," *Journal of Applied Polymer Science*, vol. 141, no. 20, p. 54782, 2024, doi: 10.1002/app.54782.

[10] M. Janda, S. Pretl, and J. Reboun, "In-situ monitoring method for curing of pastes used in printed electronics," *44th International Spring Seminar on Electronics Technology (ISSE), Bautzen, Germany*, May 2021, doi: 10.1109/isse51996.2021.9467541.

[11] S. Merilampi, T. Laine-Ma, and P. Ruuskanen, "The characterization of electrically conductive silver ink patterns on flexible substrates," *Microelectronics Reliability*, vol. 49, no. 7, pp. 782–790, May 2009, doi: 10.1016/j.microrel.2009.04.004.

[12] M. N. Zainal, R. K. Khirotdin, S. N. E. Eraman, M. F. N. Suhaimi, and N. Hassan, "Investigation of curing process of silver conductive ink on polymer substrates using halogen lamp and oven," in *Lecture notes in electrical engineering*, 2022, pp. 387–397. doi: 10.1007/978-981-19-1577-2_29.

[13] N. M. A. Salim *et al.*, "Effect of GNP/AG stretchable conductive ink on electrical conductivity," *Journal of Advanced Research in Applied Mechanics*, vol. 119, no. 1, pp. 1–12, Jul. 2024, doi: 10.37934/aram.119.1.112.

[14] G. Deng *et al.*, "Wideband absorber based on conductive ink frequency selective surface with polarization insensitivity and wide-incident-angle stability," *Nanomaterials and Nanotechnology*, vol. 10, p. 184798042093571, Jan. 2020, doi: 10.1177/1847980420935718.

[15] H. Tu, J. Hu, and X. Ding, "Measurement of the conductivity of screen printing films at microwave frequency employing resonant method," *Journal of Electronic Materials*, vol. 50, no. 2, pp. 521–527, Nov. 2020, doi: 10.1007/s11664-020-08594-w.

[16] J. M. Summers *et al.*, "The influence of ink chemistry on the microstructure evolution and GHZ RF response of printed AG transmission lines," *Materials*, vol. 17, no. 8, p. 1756, Apr. 2024, doi: 10.3390/ma17081756.

[17] N. S. H. Jori, N. M. A. Salim, N. nor A. Masripan, N. A. Md. Saad, and N. C. Photong, "Effect of butanol and terpinol as a solvents in GNP/SA conductive ink," *Journal of Advanced Research in Applied Mechanics*, vol. 120, no. 1, pp. 62–71, Jul. 2024, doi: 10.37934/aram.120.1.6271.

[18] B. G. Pollet and S. S. Kocha, "Using ultrasound to effectively homogenise catalyst inks: is this approach still acceptable?," *Johnson Matthey Technology Review*, vol. 66, no. 1, pp. 61–76, May 2021, doi: 10.1595/205651321x16196162869695.

[19] S. Aydoğan, M. Motasim, and B. Ali, "The novelty of silver extraction by leaching in acetic acid with hydrogen peroxide as an organic alternative lixiviant for cyanide," *Heliyon*, vol. 10, no. 2, p. e24784, Jan. 2024, doi: 10.1016/j.heliyon.2024.e24784.

[20] P. J. Nair and F. S. Thomas, "Effect of ultrathereforenication energy on dispersion stability and thermal conductivity of graphene nanofluids," *Colloids and Surfaces A: Physicochemical and Engineering Aspects*, vol. 658, p. 130817, 2023, doi: 10.1016/j.colsurfa.2023.130817.

[21] S. Luo and Q. Yang, "Natural frequency measurement of steel components by the sound signal," *Journal of Low Frequency Noise, Vibration and Active Control*, vol. 40, no. 2, pp. 993–1004, Sep. 2019, doi: 10.1177/1461348419860712.

[22] J. Zhang, Y. Tian, Z. Ren, J. Shao, and Z. Jia, "A novel dynamic method to improve first-order natural frequency for test device," *Measurement Science Review*, vol. 18, no. 5, pp. 183–192, Oct. 2018, doi: 10.1515/msr-2018-0026.

[23] N. Naik, S. Sharma, M. Patel, and R. Kumar, "Biopolymer-based carbon conductive inks for printed electronics," *Polymer Journal, 2025 (early view)*, doi: 10.1007/s00289-025-05947-5.

[24] Y. Sun, T. Zhang, and J. Yang, "Dynamic mechanical behavior of printed nanocomposite films characterized by modal analysis," *Senthereforers and Actuators A: Physical*, vol. 353, p. 114363, 2024, doi: 10.1016/j.sna.2024.114363.

BIOGRAPHIES OF AUTHORS

Khirwizam Md Hkhir is a senior lecturer in the Department of Mechanical Engineering, Politeknik Ungku Omar, Ipoh, Malaysia. He received the B.Eng. (Hons.) degree in Mechanical Engineering from Universiti Teknologi MARA (UiTM), Malaysia, in 2006, and the Master's degree in Vocational Education from Universiti Tun Hussein Onn Malaysia (UTHM) in 2008. He is currently pursuing a Ph.D. in Mechanical Engineering at Universiti Teknikal Malaysia Melaka (UTeM). His research interests include vibration analysis and conductive ink materials. He can contacted at email: khirwizam@puo.edu.my.

Nor Azmmi Masripan is an associate professor with the Faculty of Mechanical Engineering, Universiti Teknikal Malaysia Melaka (UTeM). His research interests cover tribology, surface engineering, and materials characterization, with a focus on coatings, bio-lubricants, and nanomaterials. He is an active member of UTeM's G-TRIBOE research group and has contributed extensively to international journals and conferences. His work includes studies on banana-peel-based bio-oil lubricants, diamond-like carbon (DLC) coatings, and graphene-enhanced conductive materials. He has been recognized for his advancements in sustainable lubrication technology. He can be contacted at email: norazmmi@utem.edu.my.

Chonlatee Photong is an associate professor with the Faculty of Engineering, Mahasarakham University, Thailand. He received his Ph.D. in Electrical and Electronic Engineering from the University of Nottingham, United Kingdom, in 2013. Before joining academia, he worked as a development engineer at Sony Device Technology and as a maintenance engineer at Seagate Technology in Thailand. His research interests include power electronics for renewable energy systems and electric motor drives. He has published more than 100 research papers and secured 15 research grants. He is currently the Deputy Dean for Administration at the Graduate School, Mahasarakham University, and leads the Electric Automotive and Energy Technology Research Unit. He also serves as an editor for several academic journals and is a Senior Member of IEEE. He can be contacted at email: chonlatee.p@msu.ac.th.

Alan Watson is an associate professor in high power electronics with the power electronics, machines, and control (PEMC) research group at the University of Nottingham, United Kingdom. He received his M.Eng. degree in Electronic Engineering in 2004 and his Ph.D. in Power Electronics from the same university. Since 2008, he has been involved in research on high-power resonant converters, high-voltage power supplies, and multilevel converters for grid-connected applications such as HVDC and FACTS systems. His current research interests include advanced high-power conversion topologies, control systems for power converters, and future energy networks, particularly VSC-HVDC technologies. He also teaches courses on electrical energy conditioning and supervises undergraduate and postgraduate research in power electronics. He can be contacted at email: alan.watson@nottingham.ac.uk.

Mohd Azli Salim is an associate professor in flexible nanoelectronics and vibro-nanotechnology with the Faculty of Mechanical and Engineering Technology, Universiti Teknikal Malaysia Melaka (UTeM), Malaysia. He earned his B.Eng. (Hons.) in Mechanical Engineering (Structure and Materials) from UTeM in 2006, an M.Eng. in Mechanical Engineering (Control Engineering) from Universiti Teknologi Malaysia in 2009, and a Ph.D. in Mechanical Engineering (Vibration Analysis) from UTeM in 2016. He is a Professional Engineer (P.Eng., Board of Engineers Malaysia), Chartered Engineer (CEng MIMechE, UK), and ASEAN Chartered Professional Engineer (ACPE-05607/MY). His research interests include finite element analysis, structural dynamics, vibration and acoustics, control engineering, and advanced nanocomposite materials. He leads research on stretchable conductive ink and electromagnetic energy harvesting at UTeM's Advanced Academia-Industry Collaboration Laboratory (AiCL). He can be contacted at email: azli@utem.edu.my.